On mesh size to cohesive zone parameters relationships

Nawfal Blal, Loïc Daridon, Yann Monerie, Stéphane Pagano

On mesh-size to cohesive zone parameters relationships

BLAL Nawfal [1,2,3] -DARIDON Loïc [1,3]
MONERIE Yann [2,3] -PAGANO Stéphane[1,3]
[1] Laboratoire de Mécanique et Génie Civil, Montpellier
[2] Institut de Radioprotection et de Sûreté Nucléaire, Cadarache
[3] Laboratoire de Micromécanique et d'Intégrité des Structures
MIST Laboratory, IRSN-CNRS-Université Montpellier 2
{nawfal.blal, loic.daridon, stephane.pagano}@univ-montp2.fr
yann.monerie@irsn.fr

November, 2011

Submitted for: Fifth International Conference on Advanced COmputational Methods in ENgineering (ACOMEN 2011)- Liège, Belgium, 14-17 November 2011

Abstract

A micromechanical model is proposed for a collection of cohesive zone models embedded between each mesh of a finite element-type discretization (cohesive-volumetric approach). The corresponding model concerns isotropic and elastic bulk behaviours and can be applied whatever the cohesive zone model, the mesh type and the triaxiality loading ratio. The overall elastic behaviour is derived using a variational approach Hashin and Shtrikman (1963); Suquet (1995) and is obtained as function of local parameters, bulk properties of relevant material and mesh density. For an isotropic discretization, a bound is obtained on the cohesive stiffnesses: the additional compliance inherent to intrinsic cohesize zone models is bounded by lower value. Others criteria on cohesive parameters (critical opening, cohesive energy, peak stress, etc.) can be obtained trough inverse analysis.

1 Introduction

The cohesive approaches had emerged as one of the most efficient methods to simulate numerical fracture processes from crack initiation to overall failure. However, their numerical implementation exhibits a strong mesh sensitivity which is still an issue of concern: it is shown in Tijssens et al. (2000) that the fracture paths depend on the mesh geometry and size. Despite this path sensitivity, the authors show that the overall force-displacement response is not very sensitive to the mesh size and can be predicted with reasonable accuracy. Another aspect of this mesh sensitivity concerns the intrinsic Cohesive Zone Models (CZM), i.e. traction-separation laws with initial slope: embedding cohesive zone models along each element boundaries leads to an additional compliance since the density of the cohesive interfaces increases as the mesh is refined.

Following Song et al. (2006), this artificial compliance can be illustrated on a simple 1D example (see Figure 1). In that case, the equilibrium condition reads: $F/S = E^M\boldsymbol{\varepsilon} = C_{\mathsf{N}}[\![\boldsymbol{u}]\!]$, where F is the applied force, $\boldsymbol{\varepsilon}$ the strain in the bulk elements (mesh size L_{mesh}, section S), E^M the Young modulus used in the bulk element constitutive behaviour, C_{N} the initial cohesive stiffness of the intrinsic model and $[\![\boldsymbol{u}]\!]$ is the displacement jump across the cohesive zone. From the definition of the overall strain $\widetilde{\boldsymbol{\varepsilon}} = \frac{F/S}{E^M} + \frac{F/S}{C_{\mathsf{N}}L_{\mathsf{mesh}}}$, one can deduce the normalized apparent Young modulus:

$$\frac{\widetilde{E}}{E^M} = \frac{F/S}{E^M\boldsymbol{\varepsilon}} = \frac{\xi}{1+\xi} \quad \text{with} \quad \xi = \frac{C_{\mathsf{N}}L_{\mathsf{mesh}}}{E^M}. \tag{1}$$

According to this last equation, the ratio ξ seems to be the key parameter of controlling the mesh sensitivity in intrinsic CZMs. More precisely, the added compliance vanishes ($\widetilde{E} \to E^M$) when $\xi \to +\infty$, see Figure 1 right. In other words, the overall elastic behaviour is not affected by the introduction of intrinsic CZMs between bulk elements and therefore the mesh sensitivity effect vanishes.

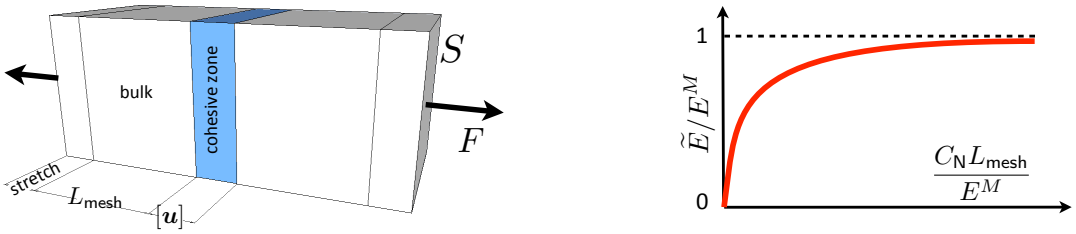

Figure 1: Illustration of the relationship between apparent Young modulus and mesh size in 1D-case: (left) a representative part of 1D finite element mesh with embedded cohesive zone model, (right) overall Young modulus normalized by bulk modulus vs mesh size.

Following the same type of ideas, various authors have proposed semi-empirical bounds for the ratio $\frac{C_{\mathsf{N}}L_{\mathsf{mesh}}}{E^M}$ in order to define 'invisible' CZMs at the scale of a structure. Performing numerical tension and shear tests, Espinosa and Zavattieri (2003) have noticed that the elastic wave speeds are unchanged across a cohesive line between two elastic and isotropic media when $\frac{C_{\mathsf{N}}L_{\mathsf{mesh}}}{E^M} \geq 10$. Estimating the added compliance for cross-triangle elements arranged in quadrilateral pattern submitted to uniaxial tension, biaxial uniform tension and pure shear, Tomar et al. (2004) obtain: $\frac{C_{\mathsf{N}}L_{\mathsf{mesh}}}{E^M} \geq \frac{\sqrt{2}+1}{\kappa(1-\nu^M)}$ with $\kappa = 1$ for plane stress and $\kappa = 1/(1-(\nu^M)^2)$ for plane strain, where ν^M is the Poisson ratio of the bulk material.

In this note, these criteria are generalized to three dimensional situations and to any type of loadings. On the other hand, the extension of the study to non linear damageable cohesive laws allows to derive an elliptic micromechanical damage model for brittle materials and exhibits others criteria on the cohesive parameters: critical opening, peak stress, cohesive energy, etc. The derived damage model does not use 1D damageable cohesive interfaces (Daridon et al. (2011)); nor is it limited to particular cohesive law (Li and Wang (2004)).

2 Linear micromechanical model

2.1 Cohesive-volumetric discretization as a 'matrix-inclusion' composite

Consider a cohesive-volumetric finite element discretization: each volumetric element is connected to each other using CZMs as boundary conditions. The main idea is to replace this discretization by a continuous *matrix* containing penny-shaped cohesive *inclusions* (Figure 2). The matrix has the same behaviour as the bulk finite element one whereas the penny-shaped

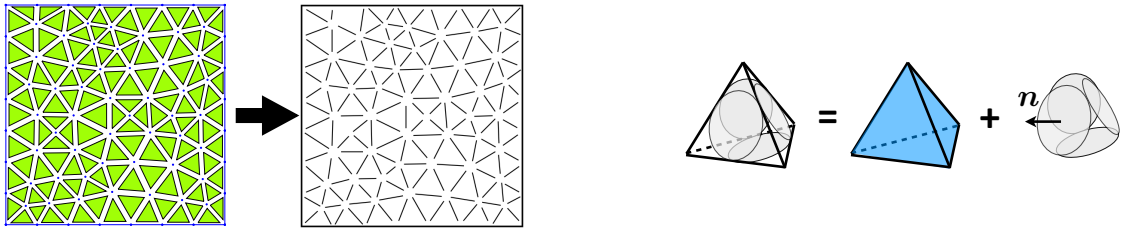

Figure 2: Principle of the approach: a cohesive-volumic finite element mesh is replaced by a continuous matrix corresponding to bulk elements and a collection of penny-shaped cohesive inclusions corresponding to the edges of the underlying mesh; (left) 2-D illustration, (right) 3-D illustration.

inclusions have a cohesive behaviour defined by a traction-separation law. The spatial distribution of the cohesive inclusions corresponds to those of the edges of the underlying mesh and has the same spatial density, denoted by Z. In particular, in the case of a statistical isotropic mesh, e.g. a Delaunay-type mesh, the inclusions are randomly distributed in space and in orientation. The shape of the inclusions is assumed to be of penny-shaped type, which corresponds to no thickness wiskers in two dimensions. The aim is to obtain the overall equivalent behaviour of such composite material using a Hashin-Shtrikman estimate Hashin and Shtrikman (1963).

2.2 Phases properties

In the sequel, we limit ourselves to linear elastic behaviours. Moreover, the matrix phase is considered as isotropic and its constitutive relation reads:

$$\boldsymbol{\sigma} = \mathbb{C}^{\mathsf{M}} : \boldsymbol{\varepsilon} \quad \text{with} \quad \mathbb{C}^{\mathsf{M}} = 3k^M \mathbb{J} + 2\mu^M \mathbb{K}, \tag{2}$$

where $\boldsymbol{\sigma}$ (resp. $\boldsymbol{\varepsilon}$) is the stress (resp. strain) field, $\mathbb{C}^{\mathsf{M}}$ is a fourth order stiffness tensor, k^M and μ^M are the bulk and the shear modulus respectively. The symmetric tensors $\mathbb{J}$ and $\mathbb{K}$ define the generic basis of the fourth order isotropic symmetric tensors: $\mathbb{J} = (1/3)\boldsymbol{i} \otimes \boldsymbol{i}$, $\mathbb{K} = \mathbb{I} - \mathbb{J}$, $2\mathbb{I}_{ijkl} = (\boldsymbol{i}_{ik}\boldsymbol{i}_{jl} + \boldsymbol{i}_{il}\boldsymbol{i}_{jk})$, $\boldsymbol{i}$ being the second order identity tensor. Initially, the cohesive constitutive law is supposed to be elastic (intrinsic model). The traction-seperation law corresponds to a linear relation between the cohesive stress vector $\mathbf{R}^{\mathsf{coh}}$ and the opening vector $[\![\boldsymbol{u}]\!]$, in a local normal-tangent basis oriented by the normal vector $\boldsymbol{n}$ to the cohesive inclusion:

$$\mathbf{R}^{\mathsf{coh}} = \boldsymbol{K} \cdot [\![\boldsymbol{u}]\!] \quad \text{with} \quad \boldsymbol{K} = \left(C_{\mathsf{N}} \boldsymbol{n} \otimes \boldsymbol{n} + C_{\mathsf{T}} \frac{\boldsymbol{u}_{\mathsf{T}} \otimes \boldsymbol{u}_{\mathsf{T}}}{\boldsymbol{u}_{\mathsf{T}} \cdot \boldsymbol{u}_{\mathsf{T}}} \right), \tag{3}$$

where C_{N} (resp. C_{T}) is the normal (resp. tangential) initial 'stiffness' of the cohesive law, u_{N} (resp. $\boldsymbol{u}_{\mathsf{T}}$) is the normal (resp. tangential) component of $[\![\boldsymbol{u}]\!] = u_{\mathsf{N}}\boldsymbol{n} + \boldsymbol{u}_{\mathsf{T}}$. The cohesive stress tensor is given combining (3) and $\mathbf{R}^{\mathsf{coh}} = \boldsymbol{\sigma}^{\mathsf{coh}} \cdot \boldsymbol{n}$ (Acary and Monerie (2006)):

$$\boldsymbol{\sigma}^{\mathsf{coh}} = \left(C_{\mathsf{N}}\mathbb{E}_l + C_{\mathsf{T}}\mathbb{K}_l\right)\left([\![\boldsymbol{u}]\!] \otimes_s \boldsymbol{n}\right), \tag{4}$$

where $\otimes_s$ is the symmetric dyadic product ($2\boldsymbol{a} \otimes_s \boldsymbol{b} = a_i b_j + a_j b_i$ for any vector $\boldsymbol{a}$ and $\boldsymbol{b}$) and $\mathbb{E}_l$, $\mathbb{K}_l$ are two components of the fourth order transversely isotropic and symmetric tensors: $\mathbb{E}_l = \boldsymbol{n}\otimes\boldsymbol{n}\otimes\boldsymbol{n}\otimes\boldsymbol{n}$ and $\mathbb{K}_l = 2(\boldsymbol{j_s}\otimes\boldsymbol{j_s} + \boldsymbol{j_t}\otimes\boldsymbol{j_t})$ with $\boldsymbol{j_s} = \boldsymbol{n}\otimes_s\boldsymbol{s}$ and $\boldsymbol{j_t} = \boldsymbol{n}\otimes_s\boldsymbol{t}$, where $\boldsymbol{s}$ and $\boldsymbol{t}$ are two orthogonal vectors defining the transversal plane ($\boldsymbol{n}, \boldsymbol{t}, \boldsymbol{s}$ define the local orthogonal basis of the cohesive inclusion). The rescaling requires to define the strain over the cohesive phase through a fictitious thickness e intended to tend toward to 0 Michel et al. (1994):

$$\boldsymbol{\varepsilon}^{\mathsf{coh}} = \frac{[\![\boldsymbol{u}]\!] \otimes_s \boldsymbol{n}}{e}. \tag{5}$$

and therefore to construct a fourth order stiffness tensor $\mathbb{C}^{\mathsf{coh}}$ leading to the following constitutive relationship for inclusions:

$$\boldsymbol{\sigma}^{\mathsf{coh}} = \mathbb{C}^{\mathsf{coh}} : \boldsymbol{\varepsilon}^{\mathsf{coh}} \quad \text{with} \quad \mathbb{C}^{\mathsf{coh}} = e\left(C_{\mathsf{N}}\mathbb{E}_l + C_{\mathsf{T}}\mathbb{K}_l\right). \tag{6}$$

Again, the parameter e is a fictitious thickness that should tend to zero. Since oblate ellispoids tend to penny-shaped inclusions when their thickness tends to zero, the cohesive inclusions are now considered as oblate ellipsoids and their volume fraction f is the product of the density Z (inversely propotional to a length: the mesh size L_{mesh}) and the fictitious thickness e: $f = eZ$ (cylindrical hypothesis instead of oblate one without any consequence when $e \to 0$).

2.3 Hashin-Shtrikman estimate

A Hashin-Shtrikman estimate Hashin and Shtrikman (1963) is used to establish an analytical expression of the overall elastic stiffness $\mathbb{C}^{\mathsf{hom}}$. This variational representation is based on the use of polarization fields related to a homogeneous reference medium (stiffness $\mathbb{C}^0$). In the case of a biphasic medium, the Hashin-Shtrikman estimate can be expressed as:

$$\mathbb{C}^{\mathsf{HS}}(\mathbb{C}^0) = \left[f\mathbb{C}^{\mathsf{coh}} : \mathbb{T} + (1-f)\mathbb{C}^{\mathsf{M}}\right] : \left[f\mathbb{T} + (1-f)\mathbb{I}\right]^{-1}. \tag{7}$$

where the fourth order tensor $\mathbb{T}$ is given by $\mathbb{T} = (\mathbb{C}^* + \mathbb{C}^{\mathsf{coh}})^{-1} : (\mathbb{C}^* + \mathbb{C}^{\mathsf{M}})$ with $\mathbb{C}^*$ being the Hill influence tensor which depends on the shape of the inclusions and on the reference medium $\mathbb{C}^0$.

3 Effective overall moduli for the elastic problem

The final expression of the Hashin-Shtrikman estimate depends on the choice of the reference medium ($\mathbb{C}^0$) and an appropriate average over mesh orientations (see Blal et al. (2011) for details). Assuming that the orientations of inclusions have the equi-probability property, which

corresponds to the case of isotropic meshes (e.g. Delaunay-type meshes), the expression (7) is reduced to (Blal et al. (2011)):

$$\mathbb{C}^{\mathsf{HS}}(\mathbb{C}^0) = \left[eZ\left\langle \mathbb{C}^{\mathsf{coh}} : \mathbb{T}\right\rangle_{\circlearrowleft} + (1-eZ)\mathbb{C}^{\mathsf{M}}\right] : \left[eZ\langle\mathbb{T}\rangle_{\circlearrowleft} + (1-eZ)\mathbb{I}\right]^{-1} \tag{8}$$

where $\langle . \rangle_{\circlearrowleft}$ indicates the average over all orientations. Following Gatt et al. (2005), this orientational average is calculating as $\langle\mathbb{D}\rangle_{\circlearrowleft} = (\mathbb{J} :: \mathbb{D})\mathbb{J} + (1/5)(\mathbb{K} :: \mathbb{D})\mathbb{K}$ for any fourth order tensor $\mathbb{D}$, and the overall stiffness tensor is obtained: $\mathbb{C}^{\mathsf{hom}} = \lim_{e\to 0} \mathbb{C}^{\mathsf{HS}}(\mathbb{C}^0)$. According to the choice of the reference medium $\mathbb{C}^0$, different bounds and estimates can be derived. Since, in a quadratic sense, the tensor $\mathbb{C}^{\mathsf{coh}}$ is smaller than $\mathbb{C}^{\mathsf{M}}$ when e tends to 0, the lower bound of the Hashin-Shtrikman estimate is obtained for the case $\mathbb{C}^0 = \mathbb{C}^{\mathsf{coh}}$:

$$\mathbb{C}^{\mathsf{hom}} = \lim_{e\to 0} \mathbb{C}^{\mathsf{HS}\text{-}}\left(\mathbb{C}^{\mathsf{coh}}\right) = \lim_{e\to 0}\left[eZ\left\langle \mathbb{C}^{\mathsf{coh}} : \mathbb{T}\right\rangle_{\circlearrowleft} + (1-eZ)\mathbb{C}^{\mathsf{M}}\right] : \left[eZ\langle\mathbb{T}\rangle_{\circlearrowleft} + (1-eZ)\mathbb{I}\right]^{-1}. \tag{9}$$

Thus, after passage to limit $e \to 0$, the overall bulk and shear moduli are:

$$\frac{k^{\mathsf{hom}}}{k^M} = \frac{\xi^{\mathsf{k}}}{\xi^{\mathsf{k}}+1} \quad \text{with} \quad \xi^{\mu} = \frac{C_{\mathsf{N}}}{Zk^M} \quad \text{and} \quad \frac{\mu^{\mathsf{hom}}}{\mu^M} = \frac{\xi^{\mu}}{\xi^{\mu}+1} \quad \text{with} \quad \xi^{\mu} = \frac{15}{4(1+3C_{\mathsf{N}}/C_{\mathsf{T}})}\frac{C_{\mathsf{N}}}{Z\mu^M}, \tag{10}$$

more practically in terms of Young modulus and Poisson ratio:

$$\frac{E^{\mathsf{hom}}}{E^M} = \frac{\xi_{\mathsf{E}}}{1+\xi_{\mathsf{E}}} \quad \text{where} \quad \xi_{\mathsf{E}} = \frac{5}{1+(4/3)(C_{\mathsf{N}}/C_{\mathsf{T}})} \times \frac{C_{\mathsf{N}}}{E^M Z}, \tag{11}$$

$$\frac{\nu^{\mathsf{hom}}}{\nu^M} = \frac{E^M Z(-1+2C_{\mathsf{N}}/C_{\mathsf{T}}) + 15C_{\mathsf{N}}\nu^M}{E^M Z(3+4C_{\mathsf{N}}/C_{\mathsf{T}})\nu^M + 15C_{\mathsf{N}}\nu^M}. \tag{12}$$

These lower bounds (10) give indication on the lost of global stiffnesses, e.g.:

$$\begin{cases} k^{\mathsf{hom}}/k^M \geq 0.95 \text{ is insured for } \xi^{\mathsf{k}} \geq 20\,, \\ \mu^{\mathsf{hom}}/\mu^M \geq 0.95 \text{ is insured for } \xi^{\mu} \geq 20\,. \end{cases} \tag{13}$$

Using the software XPER Perales et al. (2008), the accuracy of these bounds is tested for the particular case $C_{\mathsf{N}} = C_{\mathsf{T}}$ in Figure 3. As shown in Figure 3, relations (10) are lower bounds for isotropic meshes (Delaunay) and can be considered as convenient estimate for regular meshes. Moreover, it is clearly shown that criteria $\xi^{\mathsf{k}} \geq 20$ and $\xi^{\mu} \geq 20$ (dashed lines) ensure that the overall elasticity is disturbed by less than 5%.

4 Extension to the damage problem

4.1 Problem formulation

In this section, the overall behaviour for the damage part is studied (non linear damageable cohesive zone models). The macroscopic associated stress $\boldsymbol{\Sigma}$ is obtained via the constitutive law: $\boldsymbol{\Sigma} = \mathbb{C}^{\mathsf{hom}} : \mathbf{E}$. The homogeneous stiffness tensor $\mathbb{C}^{\mathsf{hom}}$ is estimated using the modified secant method Suquet (1995), which is equivalent to the Ponte Castañeda variational approach

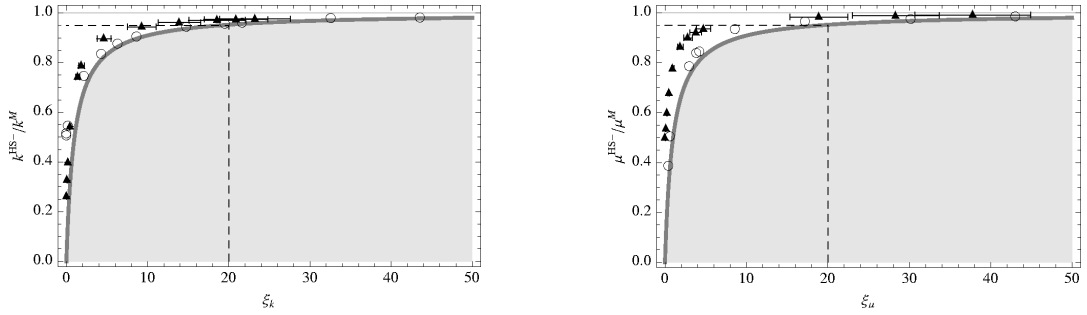

Figure 3: Normalized overall elastic modulus of a cohesive-volumetric formulation with intrinsic CZMs (case $C_{\mathsf{N}} = C_{\mathsf{T}}$): lower bounds (10) (thick gray line), numerical results for Delaunay meshes (closed symbols with variance) and for cross-triangle quadrilateral meshes (open symbols); bulk modulus (left) and shear moduls (right).

Ponte Castañeda and Suquet (1998). Focusing on the case of isotropic local damage, the non linear damageable cohesive law is defined introducing a surface damage parameter β in (3) ($\beta = 1$ the cohesive zone is undamaged, $0 < \beta < 1$ cohesive zone is partially damaged and $\beta = 0$ the cohesive zone is fully damaged), namely:

$$\mathbf{R}^{\mathsf{coh}} = \beta \times \left(C_{\mathsf{N}} \boldsymbol{n} \otimes \boldsymbol{n} + C_{\mathsf{T}} \frac{\boldsymbol{u}_{\mathsf{T}} \otimes \boldsymbol{u}_{\mathsf{T}}}{\boldsymbol{u}_{\mathsf{T}} \cdot \boldsymbol{u}_{\mathsf{T}}} \right) [\![\boldsymbol{u}]\!]. \tag{14}$$

We assume that the parameter β depends only on the norm of the displacement jump vector $[\![\boldsymbol{u}]\!]$ ($\beta = \beta(\|[\![\boldsymbol{u}]\!]\|)$). Hence, equation (14) leads to the non linear stiffness of the inclusions given by the secant modulus:

$$\mathbb{C}^{\mathsf{coh}}_{\mathsf{sct}} = \beta(\|[\![\boldsymbol{u}]\!]\|) \times \mathbb{C}^{\mathsf{coh}}. \tag{15}$$

The secant stiffness $\mathbb{C}^{\mathsf{coh}}_{\mathsf{sct}}$ replaces the cohesive tensor $\mathbb{C}^{\mathsf{coh}}$ in Hashin-Shtrikman estimate (9). Using the strain definition (5), the norm of the displacement jump $\|[\![\boldsymbol{u}]\!]\|$ can be linked to the fourth order tensor $\mathfrak{e} = (1/2)\boldsymbol{\varepsilon} \otimes \boldsymbol{\varepsilon}$ as:

$$\|[\![\boldsymbol{u}]\!]\|^2 = 2e^2(-\mathbb{J} + 2\mathbb{K}) :: \mathfrak{e}. \tag{16}$$

On the other hand, the second moment of the strain in the inclusion phase $\langle \mathfrak{e} \rangle_I$ can be linked to the overall elastic energy by (see Kreher (1990)):

$$\langle \mathfrak{e} \rangle_I = \frac{1}{2eZ} \frac{\partial(\mathbf{E} : \mathbb{C}^{\mathsf{hom}} : \mathbf{E})}{\partial \mathbb{C}^{\mathsf{coh}}_{\mathsf{sct}}}. \tag{17}$$

Hence, substituting (17) into (16), the quadratic average of the displacement jump reads:

$$\sqrt{\langle \|[\![\boldsymbol{u}]\!]\|^2 \rangle_I} = \sqrt{\frac{e}{Z}(-\mathbb{J} + 2\mathbb{K}) :: \frac{\partial(\mathbf{E} : \mathbb{C}^{\mathsf{hom}} : \mathbf{E})}{\partial \mathbb{C}^{\mathsf{coh}}_{\mathsf{sct}}}} \tag{18}$$

which may be also written involving the hydrostatic part of the strain load $\mathrm{E}_{\mathsf{m}} = (1/3)\,\mathrm{tr}(\mathbf{E})$ and the equivalent part $\mathrm{E}_{\mathsf{eq}} = \sqrt{(2/3)\mathbf{E}_{\mathsf{dev}} : \mathbf{E}_{\mathsf{dev}}}$ (with $\mathbf{E}_{\mathsf{dev}}$ being the deviatoric strain tensor:

$\mathbf{E}_{\mathsf{dev}} = \mathbf{E} - \mathrm{E}_{\mathsf{m}}\boldsymbol{i}$):

$$\sqrt{\langle \|[\![\boldsymbol{u}]\!]\|^2 \rangle_I} = \left[\frac{\mathrm{E}_{\mathsf{eq}}^2}{(1+\nu)^2(2+\nu)} + \frac{20\mathrm{E}_{\mathsf{m}}^2}{23+17\nu-44\nu^2-164\nu^3} \right]^{\frac{1}{2}} \times \mathcal{F}, \tag{19}$$

where the scalar $\mathcal{F}$ depends on the damage parameter, the cohesive stiffnesses, the material properties and the mesh size (its expression is too complicated to be given here in a closed-form). Finally, the expression of the secant modulus is given by:

$$\begin{cases} \mathbb{C}_{\mathsf{sct}}^{\mathsf{coh}} = \beta \times (C_{\mathsf{N}}\mathbb{E}_l + C_{\mathsf{T}}\mathbb{K}_l), \\ \beta = \beta \left(\left[\frac{\mathrm{E}_{\mathsf{eq}}^2}{(1+\nu)^2(2+\nu)} + \frac{20\mathrm{E}_{\mathsf{m}}^2}{23+17\nu-44\nu^2-164\nu^3} \right]^{\frac{1}{2}} \times \mathcal{F} \right). \end{cases} \tag{20}$$

Given the expression of the damage function β, one can obtain the solution of the non linear problem (20) using a numerical method, e.g. fixed point schemes. The obtained result defines therefore a micromechanical damage model applicable whatever the triaxiality loading ratio. The case of a bilinear cohesive law will be discussed in the next section.

4.2 Application: bilinear cohesive law

Focusing on the case of brittle fracture in elastic materials, a bilinear cohesive damageable law is studied hereafter (see Figure 4). An elliptic damage model is thus derived (Figure 6 left). For

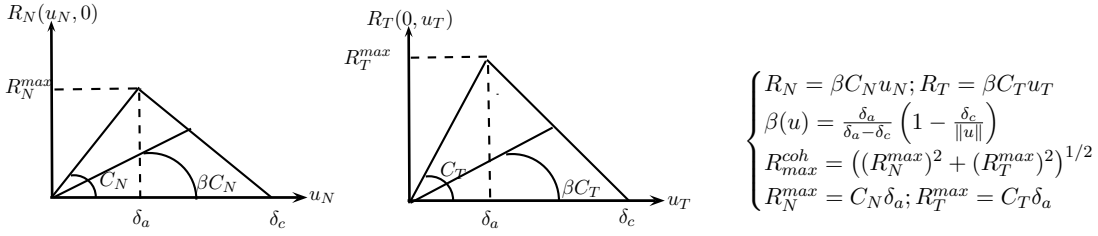

Figure 4: Cohesive bilinear law

that specific case of cohesive law, the effective yielding surface at failure is given involving the hydrostatic and equivalent strain by the equation:

$$\Psi(\mathrm{E}_{\mathsf{m}}, \mathrm{E}_{\mathsf{eq}}) = \frac{\mathrm{E}_{\mathsf{eq}}^2}{\overline{\mathrm{E}_{\mathsf{eq}}}^2} + \alpha \frac{\mathrm{E}_{\mathsf{m}}^2}{\overline{\mathrm{E}_{\mathsf{eq}}}^2} - 1 = 0 \tag{21}$$

where $\overline{\mathrm{E}_{\mathsf{eq}}} = \sqrt{10}(1+\nu^M)Z\delta_c/3(\sqrt{23+63\nu^M+82(\nu^M)^2}$ is the equivalent macroscopic strain at failure under pure deviatoric load. The coefficient α is equal to the square of the ratio between equivalent strain $\overline{\mathrm{E}_{\mathsf{eq}}}$ and hydrostatic one $\overline{\mathrm{E}_{\mathsf{m}}}$ at failure, and depends only on the Poisson ratio of the matrix ν^M (Figure 5 illustrates the effect of the Poisson ratio on the triaxilaty ratio at the failure: the more incompressible the material is, the larger the coefficient α becomes). It gives an idea about the triaxiality ratio effect associated to our model. For a material with

$E^M(\mathsf{GPa})$	ν^M	$R^{\mathsf{coh}}_{\mathsf{max}}(\mathsf{MPa})$	$\delta_c(\mathsf{mm})$	$C_{\mathsf{N}}(=C_{\mathsf{T}})(\mathsf{MPa/mm})$
340	0.3	500	10^{-5}	34.10^9

Table 1: Material and cohesive parameters

$\nu^M = 0.3$, α is about 3.94, in other words, the equivalent strain which leads to total failure, in the case of deviatoric load, is nearly twice the hydrostatic strain for a 3D traction: $\overline{\mathsf{E_{eq}}} \simeq 2\overline{\mathsf{E_m}}$ (Figure 6). Obviously, the model depends on the Poisson ratio and deals with any type of

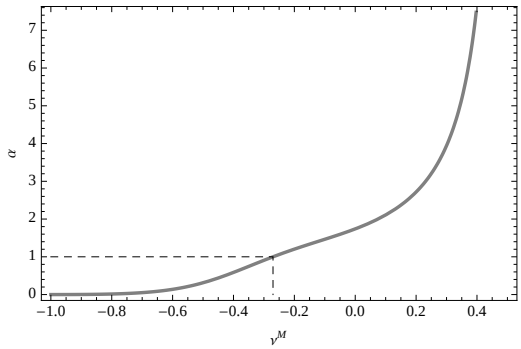

Figure 5: Triaxialty dependence on the Poisson ratio.

triaxiality. Therefore, it extends to the brittle case Gurson-like model Gurson (1977) (where no dependence to Poisson ratio can be predicted) and Li-Wang model Li and Wang (2004) (restricted to hydrostatic loads). Moreover, equation (21) and Figure 5 show that the cohesive-volumetric finite element method predicts that: 1) it is easier to break a material under purely hydrostatic loadings than under purely deviatoric ones, when $-0.27 \leq \nu^M < 0.5$, 2) it is easier to break a material under purely deviatoric loadings than under purely hydrostatic ones, when $-1 \leq \nu^M < 0.27$.

Figure 6 (right) illustrates the evolution of the macroscopic behaviour associated to the bilinear cohesive law. Results are given for the case of a pure deviatoric load and shows a dependence on the mesh size L_{mesh}. This mesh sensitivity could be avoided according to rigorous calibration of the cohesive parameters. This point is developed in details in section 5.2. The material properties and cohesive parameters are given in Table 1.

5 Inverse identification and rigorous criteria on cohesive parameters

5.1 Lower bounds on cohesive stiffness

The inverse study of the results obtained in the elastic part allows to derive an a priori estimate of the overall elastic reduction as function of the cohesive stiffnesses, and therefore to suitably calibrate them. Practical criteria are proposed following Acary and Monerie (2006) from the previous micromechanical model. Denoting by $R = E^{\mathsf{hom}}/E^M$ the overall reduction of the Young modulus ($R = 1$ corresponds to 'invisible' intrinsic CZMs) and according to equation (11), an

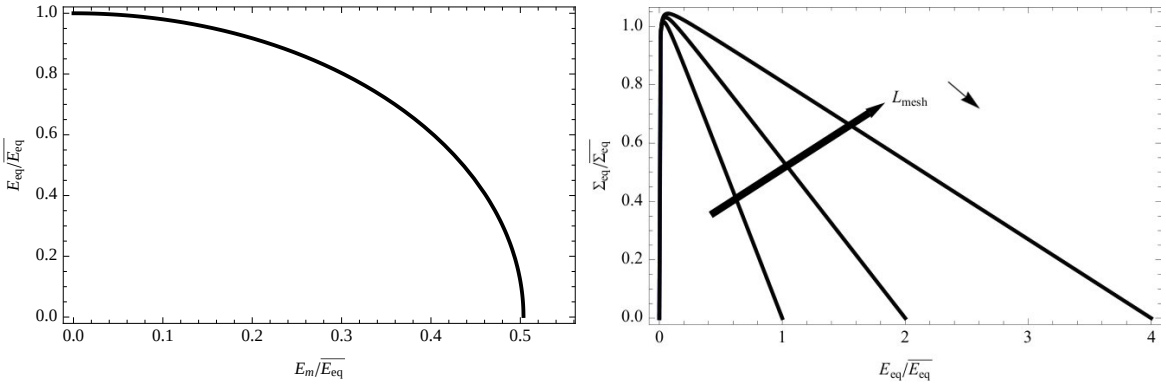

Figure 6: The elliptic damage model (21) (left) and the normalized overall behaviour for a deviatoric applied loading given different values of the mesh size L_{mesh} (right). The material and cohesive parameters are given in Table 1 and the overall stiffness reduction is tolerated at 5%, i.e. we admit that cohesive zone models disturb the overall Young modulus for less than 5%: $E^{\mathsf{hom}}/E^M = 0.95$.

implicit lower bound on $C_{\mathsf{N}}/(E^M Z)$ is obtained involving the density Z and the ratio $C_{\mathsf{N}}/C_{\mathsf{T}}$:

$$\frac{C_{\mathsf{N}}}{E^M Z} \geq \frac{1}{5}\frac{R}{1-R}\left(1+\frac{4}{3}\frac{C_{\mathsf{N}}}{C_{\mathsf{T}}}\right). \tag{22}$$

To complete the criterion (22), we suggest to ensure that the overall Poisson ratio stays equal to the matrix one: $\nu^{\mathsf{hom}} = \nu^M$. This condition leads to a restriction on the ratio $C_{\mathsf{N}}/C_{\mathsf{T}}$:

$$\nu^{\mathsf{hom}} = \nu^M \Rightarrow \frac{C_{\mathsf{N}}}{C_{\mathsf{T}}} = \frac{1}{2}\frac{1+3\nu^M}{1-2\nu^M}. \tag{23}$$

Equations (22) and (23) give a lower bound on the normal cohesive stiffness as function of the elastic reduction R: $C_{\mathsf{N}} \geq k^M Z R/(1-R)$. Since the density Z is inversely proportional to the mesh size L_{mesh}, one obtains with (22) and (23):

$$\frac{C_{\mathsf{N}} L_{\mathsf{mesh}}}{E^M} \geq \gamma \frac{R}{1-R}\frac{1}{3-6\nu^M}, \tag{24}$$

where γ depends on the spatial distribution of the considered isotropic mesh. For Delaunay meshes, γ can be represented as a mean value and a variance Stoyan et al. (1995). For non-isotropic meshes (as regular ones), we claim that the bound (24) can be considered as an accurate estimate: interestingly, the two dimensional case of 'cross-triangle quadrilateral' mesh (each square element is subdivided into four isosceles triangles) corresponds to $\gamma = 2(1+\sqrt{2})$ Acary and Monerie (2006). The bound (10) and the condition (23) allow to define a '5% criteria' ($R = 0.95$) in terms of bulk and shear moduli for 2D regular meshes:

$$\frac{C_{\mathsf{N}} L_{\mathsf{mesh}}}{k^M} \geq 92 \quad \text{and} \quad \frac{C_{\mathsf{T}} L_{\mathsf{mesh}}}{\mu^M}\left(15 - \frac{\mu^M}{k^M} L_{\mathsf{mesh}}\right) \geq 1104, \tag{25}$$

and a 'practical 5% criterion' ($R = 0.95$):

$$\frac{C_{\mathsf{N}} L_{\mathsf{mesh}}}{E^M} \geq \frac{30}{1-2\nu^M} \quad \text{with} \quad \frac{C_{\mathsf{T}}}{C_{\mathsf{N}}} = 2\frac{1-2\nu^M}{1+3\nu^M}. \tag{26}$$

5.2 Criteria on damageable cohesive parameters

The identification of the other cohesive parameters follows from the damage part: critical opening δ_c and cohesive peak value $R^{\mathsf{coh}}_{\mathsf{max}}$. Without loss of generality, interest is made for the case of overall deviatoric loads. The linearised constitutive law $\mathbf{\Sigma} = \mathbb{C}^{\mathsf{hom}} : \mathbf{E}$ gives the evolution of the macroscopic equivalent stress as function of the macroscopic equivalent strain: $\Sigma_{\mathsf{eq}}(\mathrm{E}_{\mathsf{eq}})$. The macroscopic stress is maximum when the macroscopic strain reaches the strain $\widehat{\mathrm{E}_{\mathsf{eq}}}$ corresponding to:

$$\frac{\partial \Sigma_{\mathsf{eq}}}{\partial \mathrm{E}_{\mathsf{eq}}}|_{\widehat{\mathrm{E}_{\mathsf{eq}}}} = 0, \tag{27}$$

hence, one can obtain an explicit relationship between the maximum cohesive stress $R^{\mathsf{coh}}_{\mathsf{max}}$ and the material tensile yielding stress $\hat{\Sigma} = \Sigma_{\mathsf{eq}}(\widehat{\mathrm{E}_{\mathsf{eq}}})$:

$$R^{\mathsf{coh}}_{\mathsf{max}} = \frac{\sqrt{2}\left(23 + 17\nu^M + 71(\nu^M)^2 + 151(\nu^M)^3 + 410(\nu^M)^4\right)^{\frac{1}{2}}}{3\left(1 - 2\nu^M\right)|1 + 3\nu^M|}\hat{\Sigma}. \tag{28}$$

In order to guarantee that the proposed model does not predict complete failure before the initiation of fissure opening, an additional condition concerning the choice of the critical separation δ_c is needed. For the case of regular meshes, we have:

$$\frac{\delta_c}{L_{\mathsf{mesh}}} = \frac{3\left(-1 + \sqrt{2}\right)\left(23 + 63\nu^M + 82(\nu^M)^2\right)\left(1 - 2\nu^M + 5(\nu^M)^2\right)^{\frac{1}{2}}}{\sqrt{10}\left(1 + \nu^M\right)\left(23 + 17\nu^M + 71(\nu^M)^2 + 151(\nu^M)^3 + 410(\nu^M)^4\right)^{\frac{1}{2}}} \times \frac{W}{\hat{\Sigma}}, \tag{29}$$

where W denotes the material fracture energy. The results issue from equations (23), (24), (28) and (29) give practical rules to suitably calibrate the cohesive parameters, namely the cohesive stiffnesses C_{N} and C_{T}, the maximal cohesive stress $R^{\mathsf{coh}}_{\mathsf{max}}$ and the critical separation δ_c (equivalently the cohesive energy) as function of the macroscopic material properties (E^M, ν^M) and the mesh size L_{mesh} given a user-defined stiffness reduction R. Even though these results include a dependence of the cohesive parameters on the mesh size (except the case of $R^{\mathsf{coh}}_{\mathsf{max}}$), this way to calibrate the damageable cohesive law leads to a *mesh-independent* overall behaviour: the macroscopic behaviour stays invariant regardless of the mesh size. Taking into account the previous relationships, the homogenized secant moduli are given as function of the overall load $\mathbf{E}$, where it is clearly shown that the overall macroscopic behaviour has no dependence on the mesh size:

$$\begin{cases} k^{\mathsf{hom}}_{\mathsf{sct}}(\mathbf{E}) = R\frac{(\mathrm{E}_{\mathsf{eq}}\hat{\Sigma} - 2W)}{\mathrm{E}_{\mathsf{eq}}\left(\hat{\Sigma}^2 - 6RW\mu^M\right)}k^M\hat{\Sigma} \\ \mu^{\mathsf{hom}}_{\mathsf{sct}}(\mathbf{E}) = R\frac{(\mathrm{E}_{\mathsf{eq}}\hat{\Sigma} - 2W)}{\mathrm{E}_{\mathsf{eq}}\left(\hat{\Sigma}^2 - 6RW\mu^M\right)}\mu^M\hat{\Sigma} \end{cases} \tag{30}$$

Similar results can be obtained for the case of hydrostatic loads.

6 Concluding remarks

The overall constitutive behaviour of an elastic medium with embedded cohesive inclusions has been studied. The equivalent 'matrix-inclusions' composite is considered as a representation of a cohesive-volumetric finite element modelling. As result of this micromechaical model, the following points can be highlighted:

- Rigorous lower bounds on normal, C_{N}, and tangential, C_{T}, cohesive stiffness have been obtained for isotropic meshes as well as convenient criteria for regular meshes. The accuracy of this result has been numerically checked for both Delaunay and cross-triangle quadrilateral meshes.
- The specific case of a bilinear shape cohesive zone model leads to an overall elliptic damage model for brittle materials. The approach is valid for any macroscopic triaxiality ratio and thus extends previous partial results of the literature. The proposed model is able to estimate the influence of Poisson ratio in material damage.
- All the local cohesive parameters can be linked to the overall fracture material properties at any given mesh size. One merit of the cohesive parameters inverse identification is its ability to derive an overall behaviour avoiding mesh dependency of mesh size. This result gives rigorous explications of the previous empirical results proposed in the literature.

References

Z. Hashin, S. Shtrikman, A variational approach to the theory of the elastic behaviour of multiphase materials, Journal of the Mechanics and Physics of Solids 11 (1963) 127–140.

P. Suquet, Overall properties of nonlinear composites : Secant moduli theory and its link with Ponte Castañeda's variational procedure, Comptes Rendus de l'Académie des Sciences 320 (1995) 563–571.

M. Tijssens, L. Sluys, E. van der Gissen, Numerical simulation of quasi-brittle fracture using damaging cohesive surfaces, European Journal of Mechanics A/Solids 19 (2000) 761–779.

S. Song, G. Paulino, W. Buttlar, A bilinear cohesive zone model tailored for fracture of asphalt concrete considering viscoelastic bulk material, Engineering Fracture mechanics 73 (2006) 2829–2848.

H. Espinosa, P. Zavattieri, A grain level model for the study of failure initiation and evolution in polycrystalline brittle materials. Part I: Theory and numerical implementation, Mechanics of Materials 35 (2003) 333 – 364.

V. Tomar, J. Zhai, M. Zhou, Bounds for element size in a variable stiffness cohesive finite element model, International Journal for Numerical Methods in Engineering 61 (2004) 1894–1920.

L. Daridon, B. Wattrisse, A. Chrysochoos, M. Potier-Ferry, Solving fracture problems using an asymptotic numerical method, Computers and Structures 89 (2011) 476–484.

S. Li, G. Wang, On damage theory of a cohesive medium, International Journal of Engineering Science 42 (2004) 861–885.

V. Acary, Y. Monerie, Nonsmooth fracture dynamics using a cohesive zone approach, Technical Report RR-6032, Institut National de Recherche en Informatique et en Automatique, 2006.

J.-C. Michel, P. Suquet, F. Thébaud, Une modélisation du rôle des interfaces dans le comportement des composites à matrice métallique., Revue Européenne des Eléments Finis 4 (1994) 573–595.

N. Blal, L. Daridon, Y. Monerie, S. Pagano, Criteria on the artificial compliance inherent to the intrinsic cohesive zone, Comptes Rendus de Mécanique 339 (2011) 789–795.

J.-M. Gatt, Y. Monerie, D. Laux, D. Baron, Elastic behavior of porous ceramics: application to nuclear fuel materials, Journal of Nuclear Materials 336 (2005) 145 – 155.

F. Perales, S. Bourgeois, A. Chrysochoos, Y. Monerie, Two field multibody method for periodic homogenization in fracture mechanics of nonlinear heterogeneous materials, Engineering Fracture Mechanics 75 (2008) 3378–3398.

P. Ponte Castañeda, P. Suquet, Nonlinear composites, Advances In Applied Mechanics 34 (1998) 171–302.

W. Kreher, Residual stresses and stored elastic energy of composites and polycrystals, Journal of the Mechanics and Physics of Solids 38 (1990) 115–128.

A. L. Gurson, Continum theory of ductile rupture by void nucleation and growth. Part 1 . yield criteria and flow rules for porous ductile materials, Journal of Engineering Materials and Technology 99 (1977) 2–15.

D. Stoyan, W. Kendall, J. Mecke, Stochastic geometry and its applications, John Wiley and Sons, Chichester, New York, Brisbane, Toronto, Singapore, 1995.